

# Wettability Contrast Surfaces: Fabrication and Applications

A. PEETHAN<sup>1</sup>, J. LAWRENCE<sup>2</sup> AND S.D. GEORGE<sup>1,3,\*</sup>

<sup>1</sup>*Department of Atomic and Molecular Physics, Manipal Academy of Higher Education, Manipal, Karnataka, India – 576104.*

<sup>2</sup>*Coventry School of Mechanical, Aerospace and Automotive Engineering, Faculty of Engineering, Environment and Computing, Coventry University, Gulson Road, Coventry, CV1 2JH, UK*

<sup>3</sup>*Centre for Applied Nanosciences, Manipal Academy of Higher Education, Manipal, Karnataka, India – 576104.*

Nature-inspired fabrication of surfaces with special wettability or wettability contrast is rapidly emerging as an area of intense research activity in materials research. This interdisciplinary research area of bio-mimicking naturally occurring surfaces to obtain self-cleaning, directional transport of liquids, droplet splitting, etc., have been finding an increased usage in fields such as solar cells, bio-sensing, water harvesting. This review discusses different wettability models that explain the spreading of a droplet on a solid surface, depending on the surface morphological and chemical structure. Further, we focus on the understanding of wettability contrast surfaces, its fabrication, and emerging applications in diverse areas. As elucidated here, an advancement in chemical as well as physical routes to fabricate the hierarchical structures enabled the creation of wettability contrast surfaces that exhibit contrast between superhydrophobic to superhydrophilic. In addition, the applications of desert beetle inspired wettability contrast surfaces for fog/water harvesting and other applications of surfaces with contrast wettability in the areas of microarrays, biomedical applications, and other emerging fields are reviewed in detail.

*Keywords: Bio-mimicking; Wettability; Superhydrophobicity; Superhydrophilicity; Water harvesting; Fog harvesting; Droplet assays.*

---

\*Corresponding author: e-mail: sajan.george@manipal.edu

## 1 INTRODUCTION: WETTABILITY AND MODELS

The natural competition and selection rule in the process of evolution to adapt to its environment has resulted in different kinds of surface wettability behavior for plants and animals [1, 2]. In the bionic research field, inspired by the different kinds of water spreading behavior manifested on the naturally occurring surfaces, researchers are attempting to biomimic these surfaces to achieve surfaces with desired wettability features [3-13]. The research on the biomimicking of the ubiquitous wettability behavior on various natural surfaces largely stems from their large-scale applications in diverse areas including painting, printing, chemical, and petroleum industry, etc. [14-21]. The wetting property of a solid surface is mainly characterized by the contact angle, i.e., the angle that a droplet makes between the liquid-air interface and the solid surface. The balance between the surface energies at the interfaces determine the wettability or spreading behavior of a droplet on a solid surface. The dependence on the surface energy originates from the higher energy of the surface atoms or molecules of liquids or solids as compared to interior molecules. Thus, the created surface free energy or surface tension forces cause the droplet to attain a state of minimum energy. When a droplet is in touch with a solid substrate, the attraction between the liquid molecules and the solid surface enables the achievement of minimum surface energy, often characterized by a certain contact angle value for the three-phase contact line. The surface energy of a droplet on a solid surface is less than the total of the surface free energy of two separated surfaces. The contact angle that a droplet makes on a solid surface with an ideal smooth planar and homogenous surface is characterized in terms of a balance of surface free energies, put forward by Thomas Young in 1805, given in Equation (1).

$$\cos\theta = \frac{\gamma_{SV} - \gamma_{SL}}{\gamma_{LV}} \quad (1)$$

$\theta$  is the equilibrium contact angle between the liquid and the solid surface [22].  $\gamma_{SV}$ ,  $\gamma_{SL}$  and  $\gamma_{LV}$  are the solid-vapor, solid-liquid and liquid-vapor surface tensions, respectively (Figure 1.a). The experimentally measured value of the water contact angle (WCA) determines whether the surface is water-loving (hydrophilic) or water-hating (hydrophobic). A hydrophilic surface is a surface upon which a water droplet makes a contact angle  $< 90^\circ$ . If the WCA is greater than  $90^\circ$  but less than  $150^\circ$ , the surface is called hydrophobic, whereas a surface that exhibits  $\text{WCA} > 150^\circ$  is termed a superhydrophobic surface. The superhydrophobic surfaces are further classified in terms of sliding angle or contact angle hysteresis, which is a measure of the difference in advancing and receding contact angle. The advancing contact angle is a dynamic contact angle that is measured in the process of wetting whereas dynamic receding

contact angle is measured during dewetting. The advancing contact angle accounts for the maximum contact angle that surface can have while receding contact angle quantifies minimum contact angle value, for a given droplet base area. Complete wetting, characterized by WCA $\sim 0^\circ$ , occurs for liquids with extremely low surface tension or a surface with very high surface energy. In the case of hydrophilic surfaces,  $\gamma_{SL} < \gamma_{SV}$ , the reverse is true for hydrophobic surfaces. An ideal surface that exhibits superhydrophilicity (WCA  $\sim 0^\circ$ ) can be obtained when  $\gamma_{SV} - \gamma_{SL} = \gamma_{LV}$  and an ideal surface with superhydrophobicity (WCA  $\sim 180^\circ$ ) can be obtained when  $\gamma_{SV} - \gamma_{SL} = -\gamma_{LV}$  [23]. However, it is to be noticed here that the classification of the substrate as the hydrophilic-hydrophobic boundary at WCA $=90^\circ$  is a matter of debate. Based on the attraction-repulsion forces of chemistry, Berg *et al.* suggested the boundary between hydrophilic and hydrophobic actually lies around  $65^\circ$  [24].

Real surfaces are not ideally smooth and can have certain roughness and chemical inhomogeneity that has to be taken into account while considering the contact angle. The Wenzel model accounts for the roughness of the material and the equilibrium contact angle that a droplet of water makes on a solid surface can be obtained from Equation (2).

$$\cos\theta_w = r \cos\theta \quad (2)$$

Where  $r$  is the roughness ratio, which is the ratio of the total “actual surface” area to the superficial “geometrical” surface area [25]. The roughness factor is a non-dimensional parameter with a value greater than unity. Thus, the roughness factor in the Wenzel model amplifies the intrinsic wetting properties of the sample surface (figure 1.b). This model prevails for materials with homogenous wetting or complete wetting, but with a different contact angle that stems from the additional interface, the area originated from the roughness. However, the model fails to explain wettability behavior in many situations such as substrates that are chemically heterogeneous or porous. In such circumstances, the Cassie-Baxter model is often used for describing the experimentally observed wettability behavior [26]. The Cassie-Baxter model accounts for the synergic effect of the surface roughness and chemical composition in the wetting/nonwetting properties of the solid surfaces. According to the Cassie-Baxter Model (Figure 1.c), the equilibrium contact angle can be obtained from Equation (3).

$$\cos\theta_{CB} = -1 + f_{SL}(r \cos\theta + 1) \quad (3)$$

$\theta_{CB}$  is the apparent contact angle on the Cassie – Baxter state and  $f_{SL}$  is the contact area under solid-liquid fraction. Thus, by reducing  $f_{SL}$ , it is possible to achieve  $\theta_{CB} \sim 180^\circ$ .

As compared to the Wenzel model, the entrapped air plastrons in the Cassie-Baxter state inhibit the imbibing of the water droplet and are often employed to explain the surfaces that exhibit high contact angle with low contact angle hysteresis (CAH) [27, 28]. Equation (3) can be used for homogeneous surfaces where a rough surface is covered by holes filled with water. It is pertinent to note that this state (impregnating Cassie wetting regime) (Figure 1. d) is different from the Wenzel regime, where the roughness must be filled with liquid before the drop reaches it. The Cassie-Baxter model implies that by carefully structuring the surface, it is possible to convert a hydrophilic surface to a hydrophobic surface. However, it is worthwhile to keep in mind that these classical Wenzel and Cassie equations can be proved to hold for the global minimizers of the total interfacial energy, not the local minimum in surface energy [19]. Moreover, both these models are valid for imperfect surfaces only when the droplet size is much larger than the wavelength of roughness or chemical heterogeneity [29]. The transition from a heterogeneous Cassie wetting state to an homogenous Wenzel model can happen either spontaneously or via several ways such as depositing droplets from some height, evaporation of droplets, application of an external voltage, or vibration. The dynamic pressure of raindrops ( $10^4$ - $10^5$  Pa) is much higher than the pressure to require typical Cassie to Wenzel state transition ( $\sim 300$  Pa) and the transition can occur while raindrops impinge upon a surface. The exact triggering mechanism of transition is not clear yet, as the experimental data obtained are generally controversial in nature. The transition from Wenzel to Cassie Baxter state always requires external triggers like light, heat, electric voltage, etc. In order to get further insight into the transition between these states, the Authors are encouraged to read the recent articles [30-34]. The working conditions of different kinds of micro/nanoscale structures existing in nature and its biomimicking using advanced lithographic fabrication tools has necessitated the development of the improved models. The Wenzel and the Cassie-Baxter models assume single-scale roughness, whereas a hierarchical surface exhibits dual-scale roughness (Figure 1.e). Models based on such dual-scale roughness, where nanoscale roughness is considered over the micron-scale structures, as developed Patankar *et al.* [35], exhibit a better correlation between the experimental



FIGURE 1

(a) Young Model (b) Wenzel model (c) Cassie – Baxter model (d) Cassie impregnated state and (e) hierarchical structure of wetting.

data and the naturally occurring superhydrophobic surfaces like the lotus leaf. In the model, the solid fraction in the Cassie-Baxter model depends upon the side dimension of the micron-scale square pillars  $a_1$  and the pillar spacing  $b_1$  through Equation (4).

$$f_{SL} = A_1 = \frac{1}{\left[\left(\frac{b_1}{a_1}\right) + 1\right]^2} \quad (4)$$

So that the Cassie-Baxter model then becomes:

$$\cos\theta_{CB} = -1 + A_1(\cos\theta + 1) \quad (5)$$

Similarly, the Wenzel equation becomes:

$$\cos\theta_w = \left(1 + \frac{4A_1}{a_1/H_1}\right) \cos\theta \quad (6)$$

Here  $H_1$  represents the height of the micropillars. In the Patanak *et al.* model [35], each microstructure is decorated with secondary structures of nanoscale pillars with size  $a_2$ , spacing  $b_2$ , and height  $H_2$ . By changing the subscripts of Equations (5) and (6), it is therefore possible to investigate the wetting on secondary structures.

In comparison to the classical Wenzel model and the Cassie-Baxter model, the hierarchical model explains the experimental observations of the superhydrophobic nature of many surfaces. However, many surfaces exhibit superhydrophobicity even without hierarchical structures. Of late, the models based on fractal structures are evolving to address the behavior of the surfaces that exhibit superhydrophobic, self-cleaning, and low adhesion properties [36, 37].

## 2 SURFACE WETTABILITY CONTRAST

The field of research that investigates and mimics the naturally occurring surfaces for future designs is called biomimetics (or bionics) [38]. The word biomimetics originates from the Greek word “bios” (life, nature) and “mimesis” (imitation, copy) [39]. By biomimicking naturally occurring surfaces like lotus leaves, rice leaves, gecko feet, desert beetle, cicada

wings, fish scales, etc., researchers have developed surfaces that exhibit superhydrophobicity, anisotropic wetting, wettability contrast surfaces, etc. [7, 40-48]. There are a large number of review articles that explain about the fabrication of superhydrophobic surfaces by mimicking naturally occurring surfaces such as plants (e.g., lotus leaves, taro leaves, rose petals) and animals (water strider, gecko toe, shark skin) [49-52]. Many methods like template replica, lithography, etching, sol-gel process, chemical vapor deposition, electrospinning and spraying, layer-by-layer deposition, chemical deposition, self-assembly, and laser patterning are used to fabricate these superhydrophobic surfaces [53-62]. On the other hand, on superhydrophilic surfaces, water spreads completely to form a thin flat film, and it can be used to remove the dirt or staining materials on a surface [63]. The super wetting nature of a surface is dependent on the surface energy and geometrical surface structures. Such surfaces can be fabricated using a variety of techniques like vapor deposition, phase inversion, ultrasonic spray pyrolysis, sol-gel method, self-assembly etching, electrospinning, etc. [64-66]. The advantages and disadvantages of the different techniques adopted for fabricating hydrophilic surfaces are reported in recent review articles [67, 68]. A variety of applications of superhydrophobic and superhydrophilic surfaces are already demonstrated. Recently, focus is on the fabrication of wettability contrast surfaces that control properties and functionalities [69]. As compared to the fabrication of surfaces with a single kind of wettability behavior, the fabrication of wettability contrast surfaces demands spatial modification of the surface chemistry or morphology. Inspired by the desert beetle, having a patterned superhydrophobic surface with both wettable and non-wettable regions on their back (Figure 2), researchers are now exploring to fabricate such wettability contrast surfaces for various applications including water harvesting [70]. The Namib Desert *Stenocara* beetle is capable of harvesting drinking water from fog-laden wind using its patterned wettability surface on its elytra. In the case of the desert beetle, their dorsal surface consists of alternating hydrophilic bumps (0.5 mm in diameter and separated by 0.5 – 1.5 mm distance) and hydrophobic valleys (see Figure 2). Due to this, the water droplets normally condense on the hydrophilic region, and it finally reaches the beetle's mouth through a hydrophobic valley. The hydrophilic bumps are smooth, and the valleys consist of special microstructures, which coated with wax. Wettability contrast surfaces are gaining more interest recently because the hydrophilic regions can act as surface tension confined microchannels and the discontinuous dewetting can channelize the aqueous solution into the wetting region. Additionally, the superhydrophobic areas can control bio-adhesion, and the wettability contrast can control the droplet behavior and transport [30]. Recently bio-inspired wettability contrast surfaces are extensively used for various applications like droplet assays, water harvesting, lab on a chip, etc. [71].

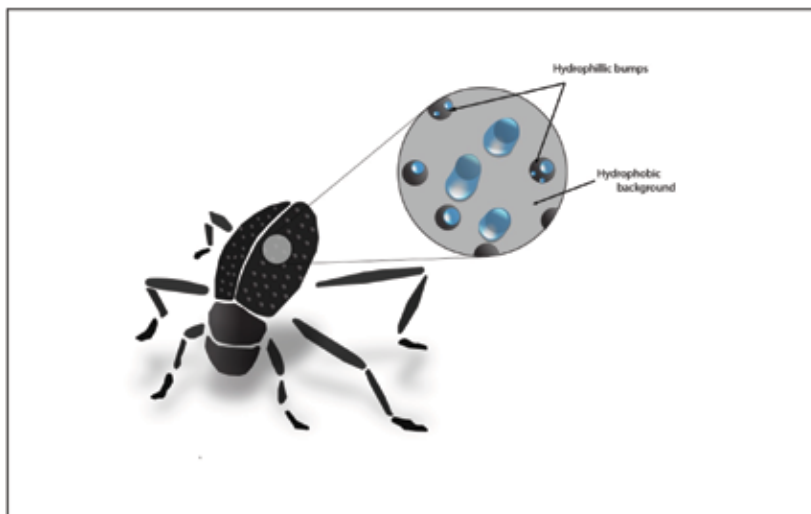


FIGURE 2  
Stenocara beetle showing hydrophilic bumps on a hydrophobic background on the elytra.

### 3 FABRICATION OF SURFACE WETTABILITY CONTRAST SURFACES

The literature on wettability contrast surfaces reports a variety of methods to tune either surface chemistry or the morphology to fabricate the required wettability contrast surfaces. Fabrication of robust and stable surfaces in a cost-effective, but via an easy route, remains a major challenge in this field. Herein, we outline a few prominent methods employed to fabricate wettability contrast surfaces.

#### 3.1 UV light irradiation

Inspired by Stenocara Beetle, Dorrer and Ruhe [72] fabricated circular hydrophilic regions on a superhydrophobic surface. Silicon nanograss with high roughness was initially fabricated using the reactive ion etching method. A monolayer of benzophenone-based silane, (4-(3'-chlorodimethylsilyl) propyloxybenzophenone) was immobilized onto the roughened silicon surface and then dipped in poly(heptadecafluorodecylacrylate) (PFA,  $c = 3 \text{ mg/mL}$  in 1,1,2-trichlorotrifluoroethane). The substrate was then irradiated with a UV light at 265 nm for 5 minutes for the covalent bonding of the polymer monolayer to the silicon. In order to generate the bumps, defined volumes of (0.5-1  $\mu\text{L}$ ) of different polymers (poly(dimethylacrylamide) (PDMAA) in ethanol, poly(styrene) (PS) in toluene, and PFA in 1,1,2-tri-

chlorotrifluoroethane) was dispensed onto the nanograss surface. The solution was then evaporated at 80°C by keeping the sample on a hot plate, and the process is repeated until circular bumps of materials are obtained. Alternatively, aluminum mask with circular openings of 500  $\mu\text{m}$ , 1 mm, 2 mm, and 5 mm in diameter can be placed onto the nanograss substrate and the ensemble irradiated with UV light of wavelength 190 nm for 2 hours, leading to a photovolatilization of the PFA surface coating in those regions not protected by the photomask.

UV light exposure was used by Takai *et al.* [73] to convert the selected regions of the superhydrophobic surfaces fabricated by depositing a mixture of trimethylmethoxysilane and Ar gas mixture onto glass and Si wafers via microwave plasma-enhanced chemical vapor deposition technique to superhydrophilic. The UV exposure caused the decomposing of the methyl group to make the irradiated region as superhydrophilic with a WCA  $\sim 0^\circ$ , whereas for the superhydrophobic region the contact angle was  $\sim 155^\circ$ . Additionally, the contact angle hysteresis in the superhydrophobic region was found to be  $\sim 4^\circ$ . In another interesting study, Levkin *et al.* [74] created a superhydrophobic-superhydrophilic microarray via UV-initiated photografting. In their method, a grid-like superhydrophobic pattern was created on a glass plate coated with a thin layer (12.5  $\mu\text{m}$ ) of superhydrophilic, biocompatible nanoporous (50% porosity, 80-250 nm pores) poly(2-hydroxyethyl methacrylate-coethylene dimethacrylate) (HEMA-EDMA). The standard esterification procedure was then adopted to modify the HEMA-EDMA layer with 4-pentynoic acid to create an intermediate alkyne surface which was then functionalized via thiol-yne click reaction by UV radiation at 260 nm (12 mWcm<sup>-2</sup>). In their approach, the extreme wettability of the microspots guaranteed easy and homogeneous adsorption of the spotting solutions, while the narrow superhydrophobic barrier effectively prevented cross-contamination of the spotting solutions between adjacent microspots. The same group also demonstrated the preparation of superhydrophilic patterns on superhydrophobic micro/nanoporous thin films via UV-initiated surface photografting where the mask determines the geometry [75]. The UV-initiated radical polymerization of a prepolymer mixture comprising of the monomers, crosslinkers, porogens, and UV-initiator was employed to make microporous poly(butyl methacrylate-co-ethylene dimethacrylate) (BMA-EDMA) films. The porous films covered with a less porous micrometer layer thin film, and it was mechanically or chemically etched to create microporous film and nanoporous film, respectively. The exposure of rough porous surface during fabrication was essential to achieve both superhydrophobic and superhydrophilic effects. The superhydrophobic property of the BMA-EDMA layer stems from the combined effect of dual-scale roughness, pores in the surface, and the hydrophobic nature of butylmethacrylate monomers. UV irradiation through the mask after wetting with a photografting mixture (methacrylate monomer, initiator benzophenone, the mixture of *tert*-butanol, and water) led to a superhydro-

philic region (if a hydrophilic methacrylate is used in the grafting mixture) with a static WCA  $\sim 0^\circ$ . In another interesting study, Sheng *et al.* [76] fabricated superhydrophobic-superhydrophilic surface on a three-layer heterostructure of TiO<sub>2</sub>/PDMS/Cu superhydrophilic surface. In their approach, the Authors spin-coated onto Cu to form a thin layer of PDMS ( $\sim 15\text{--}20\ \mu\text{m}$ ), which was then heated at  $160^\circ\text{C}$  for ten minutes. Following this, an ultrathin oxide layer ( $\sim 1\ \mu\text{m}$ ) was placed onto the PDMS film by rolling a droplet of TiO<sub>2</sub> nanoparticles (20–200 nm)-ethanol suspension. A UV LED (3W) flashlight was then used to irradiate the TiO<sub>2</sub>/PDMS/Cu at an intensity  $10\ \text{mWcm}^{-2}$  for two minutes so that the irradiated region exhibited a WCA of  $153^\circ$  as opposed to the  $6^\circ$  for the non-irradiated region.

### 3.2 Laser Treatment

An interesting study demonstrated the fabrication of wettability contrast surface via computer-controlled CO<sub>2</sub> laser treatment of surface-treated hydrophobic paper so that the selected region was converted to hydrophilic [77]. Herein, the laser power and scanning speed were controlled because the high laser power and low scanning speed led to the removal of the surface as well as the bulk of the material. In another interesting work, Wang *et al.* [78] produced a grid-shaped superhydrophilic-superhydrophobic pattern on a substrate. Figure 3 shows the schematic of the fabrication of the wettability contrast surface. Here, a substrate of hydrophilic nature is initially converted into a superhydrophobic surface via particle spray of hydrophobic silica PDMS aerosol particles. Following the drying of the substrate for 24 hours, deposition of the hydrophilic layer of Pt nanoparticles through a stainless steel mesh was carried out via pulsed laser (Nd:YAG laser, 355 nm) deposition technique. The deposition was performed at room temperature with a pressure of  $8.9 \times 10^{-4}\ \text{Pa}$  and laser power of 2W. The distance between the target and substrate was kept at 7 cm, and the deposition was carried out for 20 minutes.

In another interesting study, Domke *et al.* [79] explored the laser-assisted patterning for the fabrication of superhydrophilic-superhydrophobic micropatterns. In their research, the borosilicate glass (4-inch size with a thickness of  $500\ \mu\text{m}$ ) was irradiated with a linearly polarized femtosecond laser (520 nm) of pulse duration 380 fs and a repetition rate 200 kHz. A galvanometer-scanner was used to create a grid pattern (with an inter-pattern spacing of  $16\ \mu\text{m}$ ) by moving the Gaussian laser beam at a laser energy near to the ablation threshold ( $F_0=6.2\ \text{J/cm}^2$ ). The debris was removed by using an ultrasonic acetone bath and an isopropanol bath. The laser patterning created hierarchical structures with a hatch spacing of  $10\ \mu\text{m}$  that was equal to the hatch height but with periodic bumps and valleys with a periodicity of about 700 nm. In order to make the substrates superhydrophobic, a 50 nm thick layer of Teflon-like polymers ((CF<sub>2</sub>)<sub>n</sub>) was deposited onto the laser machined surface. To generate a wettability contrast surface, selective removal of the Teflon like

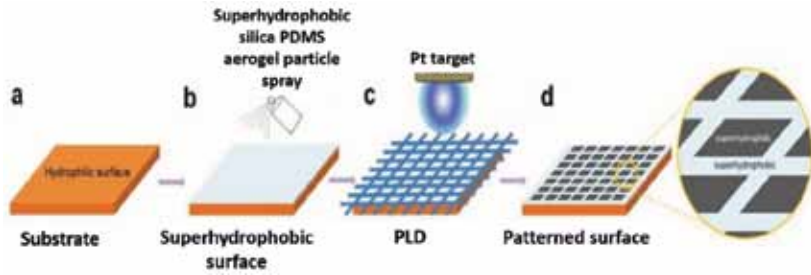


FIGURE 3

Schematic representation of the construction of the wettability contrast surface. (a) A clean substrate, (b) spraying of superhydrophobic silica PDMS aerogel on the substrate, (c) platinum deposition on a masked superhydrophobic surface using PLD approach (d) superhydrophobic/superhydrophilic patterned surface (Reprinted with permission [78]).

polymer was carried out using the femtosecond laser so that superhydrophilic spots with a diameter of 500  $\mu\text{m}$  and 1000  $\mu\text{m}$  center-to-center distance were fabricated on the superhydrophobic background.

Kietzig *et al.* [80] demonstrated the wettability modification of the porous polyethylene terephthalate (PET) microstructured surface by the incorporation of titanium nanoparticles through pulsed laser deposition. The fabrication of porous PET surfaces and pulsed laser deposition was carried out using an amplified Ti:sapphire laser which emitted a horizontally polarised Gaussian beam of 800 nm wavelength, 4 W output power, in pulses of 150 fs pulse duration, and at a repetition rate of 1 kHz. Before micromachining, the pristine PET exhibited an advancing contact angle of  $92 \pm 2^\circ$  and receding contact angle of  $57 \pm 2^\circ$ . After laser processing, the porous PET surface was more hydrophilic than the pristine PET, with advancing and receding angles of  $82 \pm 2^\circ$  and  $43 \pm 2^\circ$ , respectively. The deposition of nanoparticles at atmospheric conditions to the laser-treated surface through pulsed laser deposition, by keeping 1 mm target-substrate distance, led to the formation of the extremely hydrophilic surface.

In a recent study, femtosecond laser patterning (Wavelength: 1030 nm, Pulse duration: 800 fs, Repetition rate: 400 kHz) was carried out on a Ti surface (purity 99.99%) at a scanning speed of 1000 mm/s to create uniform microstructure square arrays [81]. Following this, the sheets were treated hydrothermally in 3 mol/L NaOH solution at 220°C for 24 hours using an electric oven. The transformation of the surface to low toxic and highly stable  $\text{TiO}_2$  was carried out by immersing the sheets in 1 mol/L HCl for 10 minutes. The distilled water washed sheets were then annealed at 450°C for 1 hour in air using a muffle furnace. In order to create wettability patterned surfaces, a thin layer of PDMS liquid spin-coated on flat silica surface was evaporated at 300°C through a mask so that hierarchical structures of PDMS exhibited

superhydrophobic behaviour whereas the other regions exhibited a hydrophilic nature.

### 3.3 Chemical Methods

In one of the early studies, Cohen *et al.* [82] tried to mimic the *Stenocara* beetle's back surface using chemical methods. The strategy that the Researchers adopted was to fabricate stable superhydrophobic coatings of rough microporous poly(allylamine hydrochloride) (PAH)/poly(acrylic) microstructures decorated with PAH/silica nanoparticles that were covered with semi-fluorosilane molecules. Then, by delivering polyelectrolytes through the semi-fluorosilane network, the local wettability properties could be tailored as the polyelectrolyte formed electrostatic bonds with the underlying PAH or silica nanoparticles, whilst keeping part of the charged polymer chains on the superhydrophobic surface. The Researchers verified the strategy by creating a hydrophilic domain using the poly(fluorescein isothiocyanate allylamine hydrochloride, FTIC-PAH) dissolved in water/2-propanol (surface tension  $21.7 \text{ mJ/m}^2$ ) in the 60/40 v/v ratio. The hydrophilic region was patterned via depositing microdrops of 1% FITC-PAH polyelectrolyte. The *Stenocara* beetle structure was mimicked by depositing an array of hydrophilic spots of  $750 \mu\text{m}$  onto a superhydrophobic surface by using a poly(acrylic acid) (PAA) water/2-propanol solution which acts as fog collecting regions.

Surfaces with different kinds of wettability patterns can be fabricated in the following procedure: Initially, a superhydrophilic surface is fabricated by depositing  $\text{TiO}_2$  slurry onto a bare silica glass via a spin-coating method, and further treatment of the surface with heptadecafluorodecyl-trimethoxysilane (FAS) changes the surface to become superhydrophobic. The UV exposure to such substrates with structures of desired features leads to a wettability patterned surfaces as the FAS-modified superhydrophobic  $\text{TiO}_2$  surface becomes superhydrophilic again due to the photocatalytic decomposition of the FAS monolayer [83]. The schematic of the fabrication of the star-shaped wettability patterned surface is illustrated in Figure 4.

In another simple but efficient approach, patterned surfaces are fabricated by exploiting the hydrophilic nature of the polydopamine coating [84]. For this, the dopamine solution (dopamine hydrochloride (2 mg/mL) dissolved in 10 mM Tris-HCl solution (pH  $\sim 8.5$ )) is simply sprayed into different hydrophobic surfaces like polypropylene (PP), polytetrafluoroethylene (PTFE), polyethylene (PE), polystyrene (PS), and polycarbonate (PC) so as to form the droplets. The droplets perform as micro-reactors, generating polydopamine thin coatings at the interface of the solid/liquid contacting area to provide the hydrophilic region. The substrate, along with the droplets is then kept in a humidity box with relative humidity (RH) of 90%. After 30 min, the substrate can be taken out and washed thoroughly to obtain hydrophilic zones on the hydrophobic background.

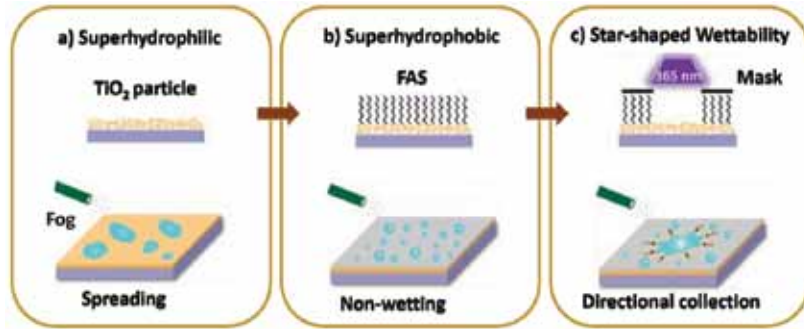


FIGURE 4

Schematic illustration of the fabrication of star-shaped wettability patterns. (a) The superhydrophilic surfaces composed of  $\text{TiO}_2$  particles and the spreading of fog droplets on it, (b) FAS coated superhydrophobic surface and nonwetting nature of fog droplets on the surface, (c) star-shaped contrast created by illuminating FAS modified surface under UV light with a photomask and directional collection of fog droplet towards the star shape region. (Reprinted with permission [78]).

In recent work, hydrophilic polystyrene flat sheet was selectively modified by incorporating a (super)hydrophobically modified copper metal-based gauze by a simple lab-based thermal processing technique [85]. Here, the copper gauzes were immersed in 4M HCl aqueous solution for a few seconds, followed by washing in a copious mixture of ethanol and deionized water. Calcination at  $400^\circ\text{C}$  for 3 hours of the cleaned substrate resulted in the production of surface copper oxide nanostructures. Following the immersion of the gauzes with black copper oxide layer into a 1.0% v/v PFDT ethanol solution for 20 minutes and subsequent washing in ethanol and drying nitrogen flow, the surface converted into hydrophobic ( $\text{CuO-x-PFDT}$ ) surface whereas the surface without calcination ( $\text{Cu-x-PDFT}$ ) exhibited an as-received, unmodified wettability behaviour. The composite sample was then prepared by keeping a piece of superhydrophobic  $\text{CuO-x-PFDT}$  on a polystyrene sheet and heated in an oven at a pre-defined temperature (i.e., 120, 130, 140, 150, and  $160^\circ\text{C}$ ) for 3 hours. Before heating in the oven, a fixed pressure was applied to superhydrophobic  $\text{CuO-x-PFDT}$  on a polystyrene sheet to keep them together.

Another exciting work demonstrates the fabrication of wettability contrast to a region as small as 290 nm on the metallic surfaces (e.g., copper) with pen drawn masks [86]. The water-resistant ink acts as a mask for the substrate so that selective patterning of nanowires and nanostructures can be made onto the exposed region via chemical oxidation and plasma deposition. After the removal of the ink, the deposition of fluorocarbon film resulted in hydrophobic/superhydrophobic patterned copper surfaces. The nanowire growth on the cleaned copper surface (via immersing in acetone, glacial acetic acid, and

native copper oxide) was achieved by immersing in a 0.1 M sodium bicarbonate and 0.02 M ammonium persulfate solution for 24 hours which was then dried in nitrogen gas. Similarly, a nanostructured aluminum alloy surface was created by immersing the plate in a 1.0 M cupric chloride solution for 5 s. Then the wettability was altered by deposition of a thin fluorocarbon layer using the parallel plate radio frequency (13.56 MHz) vacuum plasma reactor operating at 110°C and 120 W of power. The pressure was kept at 1 Torr using a mixture of pentafluoroethane (Praxair) and Argon at 20 SCCM and 75 SCCM, respectively. A deposition time of 5 s resulted in a highly cross-linked 23 ( $\pm 1$ ) nm fluorocarbon layer covalently bonded to the copper and aluminum alloy surfaces. In the case of copper foil, the patterned regions exhibited hydrophobicity with static, advancing and receding contact angles of  $110.9^\circ \pm 2.2^\circ$ ,  $123.9^\circ \pm 2.2^\circ$ , and  $86.2^\circ \pm 1.9^\circ$ , respectively, whilst super-hydrophobicity was observed on the background region with static, advancing, and receding contact angle of  $161.7^\circ \pm 2.2^\circ$ ,  $170.6^\circ \pm 2.4^\circ$ , and  $159.5^\circ \pm 1.1^\circ$ , respectively. In another interesting work, a two-step chemical etching process (superhydrophobic region by masked chemical etching and stearic acid modification and superhydrophilic region by chemical etching with dropping liquids) was proven to be efficient in fabricating the surfaces with extreme wettability patterns [87]. Initially, a mask with a designed shape was bonded to an oxide layer free aluminium plate and then etch with  $1\text{ molL}^{-1}$  of  $\text{CuCl}_2$  solution for 20 seconds to obtain micro/nanostructures. Following this, the surface was modified with  $0.05\text{ molL}^{-1}$  of ethanol solution of stearic acid to get a superhydrophobic region, whereas the masked region retained its original hydrophilicity. The dropping of  $1\text{ molL}^{-1}$  of  $\text{CuCl}_2$  on the hydrophilic region caused the etching process that resulted in the Cu particles in the spread region and subsequently made the surface superhydrophilic. In this process, the WCA of the pristine surface changed from  $72^\circ$  to  $161.5^\circ$  in the step of etching for a duration of 10 seconds and then remained nearly the same with further increased etching time. In step II, the surface became superhydrophilic with a WCA less than  $10^\circ$  for an etching period of 15 seconds. The fabricated surfaces exhibited stable extreme wettability patterns in air and underwater.

In another interesting work, to demonstrate fog collection, peripheral insulating paint on a needle was removed, to firstly convert the surface to a superhydrophilic nature by soaking it vertically in the dopamine solution (2 mg dopamine dissolve in 10 mL, pH = 8.5, Tris-(hydroxymethyl)-methylamine solution) for 4–6 h [88]. The needle was then painted with a 3% chitosan (CS) solution followed by immersing vertically into a 5% glutaraldehyde solution for 5 minutes. The modified needle was then dried in a vacuum oven at 25°C for 30 minutes. The superhydrophilic tip was then painted with melted paraffin wax to make it hydrophobic in nature. The superhydrophobic surface was obtained by burning the steel needle in a muffle over at 200°C for 30 minutes and then by covering it with 2% PVDF-HFP DMF solution before being allowed to cool. The different wettability surfaces were made by immersing

the steel needle in an aqueous solution of 2.5 M NaOH and 0.13 M  $(\text{NH}_4)_2\text{S}_2\text{O}_8$  at 25°C to achieve WCA in the range of 5° to 106°.

### 3.4 Chemical Vapor Deposition

In a study, a PET substrate was made super-water-repellent by altering the surface with annular wettable patterns [89]. The nanoscale roughened glass surface on the Ar gas cleaned substrate was achieved via  $\text{O}_2$  etching in plasma-assisted chemical vapor deposition (PACVD) chamber for 30 minutes, followed by a coating of amorphous  $\text{C}_6\text{H}_{18}\text{Si}_2\text{O}$  film using hexamethyldisiloxane (HMDSO) gas. Selective hydrophilization of an annular region was achieved after the development of a spin-coated photoresistor (AZ 1512) following UV irradiation. The treatment with air plasma on the developed substrate made the photopatterned regions superhydrophilic, and other region remained a superhydrophobic (WCA =  $160 \pm 2^\circ$  and CAH =  $5 \pm 2^\circ$ ).

In another interesting study, candle soot particles were first deposited onto a glass substrate then silica shell was coated on the candle soot particles by chemical vapor deposition of tetraethoxysilane (TEOS) [90]. Calcination at 550°C for 2 hours was carried out to get rid of the template particles leading to the silica coating with several quasi-spherical particles that form a dendritic like network. Then, the coating was immersed in an ethanol solution of octadecyltrichlorosilane (OTS) for 1 h to obtain superhydrophobic Properties with WCA  $\sim 165.5 \pm 1.1^\circ$  and a sliding angle of  $5.6^\circ$ . The superhydrophobic microwells (WCA  $\sim 0^\circ$ ) were created on this surface via UV light irradiation through a photomask for 45 minutes. Figure 5 shows the condensing-enrichment effect on a superhydrophilic microwell spotted on a superhydrophobic substrate for the fluorescent signals and the SEM images of the nanodendritic silica coating after the removal of candle soot.

The fabrication of superhydrophilic-superhydrophobic micropatterns has been achieved through the chemical vapor deposition technique also. In this case, candle soot was deposited onto a glass slide (5cm) at a speed of 5 cm/s for 9 seconds. The chemical vapor deposition of the TEOS (2mL) catalyzed by ammonia solution (2mL, 98%) in a desiccator at 37°C for 20 hours was carried out onto the candle soot deposited glass substrate to form the silica. The carbon core was then removed by calcination at 600°C for 1 hour, and the substrate became nanodendritic silica, which was then modified by OTS solution (1 vol% of anhydrous toluene) for 15 minutes. Following this, the substrates were washed with toluene and ethanol and heated at 120°C for 15 minutes and UV irradiated through a photomask for 45 minutes to fabricate the superhydrophilic microwell (exposed region)-superhydrophobic surface [91].

### 3.5 Inkjet Printing

In an approach for the fabrication of wettability contrast, by following the schematic depicted in Figure 6, a wettability contrast surface was created.

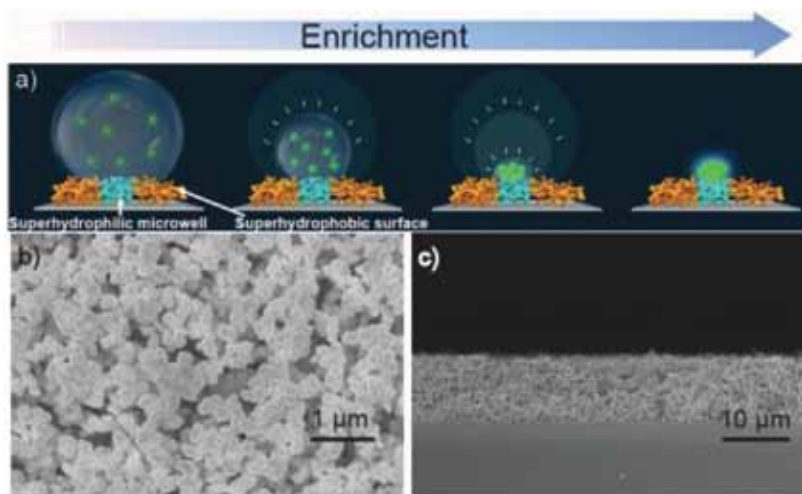


FIGURE 5

(a) Condensing-enrichment on a superhydrophilic microwell spotted on a superhydrophobic substrate, (b) top view and (c) side view SEM images of the nanodendritic silica coating after the removal of candle soot. (Reprinted with permission [85]).

Initially, the microstructured silicon carbide substrate was converted to a superhydrophobic surface by polymer/nanoparticle dispersion via a wet processing method [92]. The nanoparticle suspension was made by the following procedure: hydrophobic fumed silica (HFS; Aerosil R 9200) and acetone, mixed mechanically and sonicated (500 J of probe sonication) and then treated with acetic acid and combined with fluoroacrylic copolymer (PMC; 20 wt.% in water). The mixture was mechanically stirred at room temperature for further drop-casting on microtextured paper (1500 grit). The drop cast paper was dried in an oven to 80°C to remove residual solvent, and the wicked solution led to the formation of a hierarchically rough surface and makes the surface superhydrophobic. The hydrophilic region in the desired area was produced via inkjet printing. One layer of the following colours was applied successively to the areas desired to be hydrophilic: magenta, yellow, cyan, and gray (50% black). The regions appeared as black for multiple colour layer printed regions, whereas regions printed incorrectly appeared in their inherent colour and thus exposed a misprint. Finally, the ink was dried using a hot air gun for 30 seconds. Herein, the superhydrophobic surface exhibited a WCA  $\sim 155^\circ$  and the superhydrophilic surface exhibited a WCA  $\sim 0^\circ$ .

By exploiting the Cassie-Baxter to Wenzel wetting transition of polydopamine onto a superhydrophobic surface by reducing the surface tension and thus lowering the vapor pressure to prolong the self-polymerization to create superhydrophilic surface, wettability patterned surfaces can be created [93].

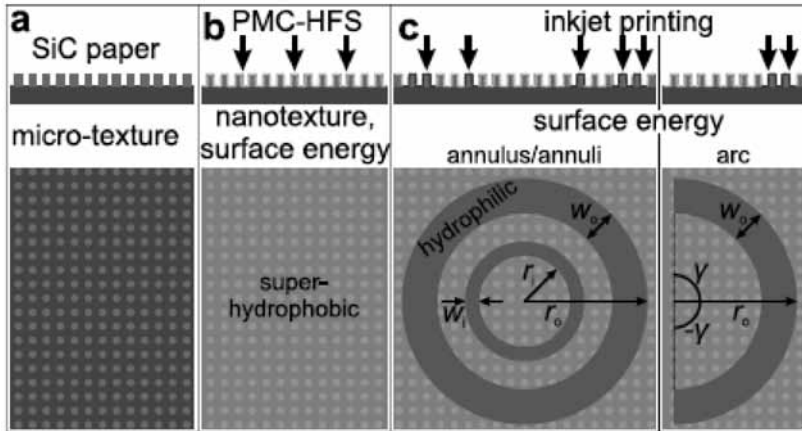


FIGURE 6

Schematic of fabrication of wettability contrast on silicon carbide surface. (reprinted with permission [92]).

The patterns are defined by direct inkjet printing of the pre-designed micropatterns onto a superhydrophobic surface. Initially, the superhydrophobic surfaces are made by following the procedure: a 1.0 g mass of the silica nanoparticles was dispersed in 30 mL of chloroform, and 1.0 g of PS granules dissolved in this dispersion by continuous stirring for 1 h. The mixture is then spin-coated onto pre-cleaned glass slides at about 1500 rpm for 60 seconds coated glass slides are then calcined in an oven at 600 °C for 2 hours and then coated with semifluorinated silane of 1H,1H,2H,2H-per-fluorooctyltriethoxysilane. To carry out the inkjet printing, dopamine solution (5.0 mgmL<sup>-1</sup>) is tris buffer solution (10Mm, PH 8.5), ethanol, and ethylene glycol (1:1: 1v/v/v) solution is filled into the cartridge to produce 10 pl in volume droplet using a Dimatrix Materials Printer. Following the printing, the substrate is then transferred to a sealed chamber and stored at 50°C for 36 h for the polymerization of dopamine and then finally washed with a copious amount of ethanol and dried under nitrogen flow.

### 3.6 Plasma Treatment

In a plasma-assisted study, the wettability contrast surfaces were made on a steel surface [94]. Different steel surfaces were first mechanically polished and then ultrasonically cleaned in ethanol and dried with nitrogen gas. The dried samples were then etched in CF<sub>4</sub> gas for a duration of between 10 to 120 minutes from a radio frequency, plasma-enhanced chemical vapor deposition system (gas pressure ~ 20 m Torr and voltage ~ 600 V<sub>b</sub>, respectively) to make the surface superhydrophobic. The surfaces were then immersed in water with a duration that varied between 10 and 120 min. To lower the surface

energy of the nanostructured surfaces, a hydrophobic material (C:H:Si:O) was deposited on each surface using a precursor of hexamethyldisiloxane (HMDSO) by PECVD (gas pressure  $\sim 10$  Torr, voltage  $\sim 400$  V<sub>b</sub> for a duration 20 seconds). The stainless steel masks with different patterns were attached to the target surface, and oxygen plasma treatment was carried out to make the exposed region superhydrophilic. A contact angle contrast of  $160^\circ$  to  $5^\circ$  was obtained between the superhydrophobic and superhydrophilic regions [94].

As depicted in Figure 7, superwettable electrochemical sensors with patterned superhydrophobic and superhydrophilic microarrays can be obtained by combining the electrochemical deposition with template oxygen plasma technology [95]. The cleaned (in ultrasonic for 10 minutes in deionized water, acetone, aqueous ammonia, and deionized water sequentially to remove organic matter and then dried with nitrogen flow) ITO surface was sputtered with a titanium layer and gold film to work as an electrode for electrochemical deposition process at room temperature. The reference and counter electrodes were made from Ag/AgCl wire and Pt wire, respectively. Gold nanodendritic structures were then electrodeposited at  $-1.8$  V for 1800 s in an electrolyte composed of HAuCl<sub>4</sub> (1 mg/mL) and sulfuric acid (0.5 M). Following the deposition, the superhydrophobic-superhydrophilic micropatterns were prepared. Firstly, an oxygen plasma at 100W was exposed onto the dendritic gold nanostructure for 180 seconds to remove organic matter and then immersed in dodecanethiol solution (10 v% in ethanol) for 24 hours and then cleaned with ethanol and ultrapure water. Then through a photomask, oxygen

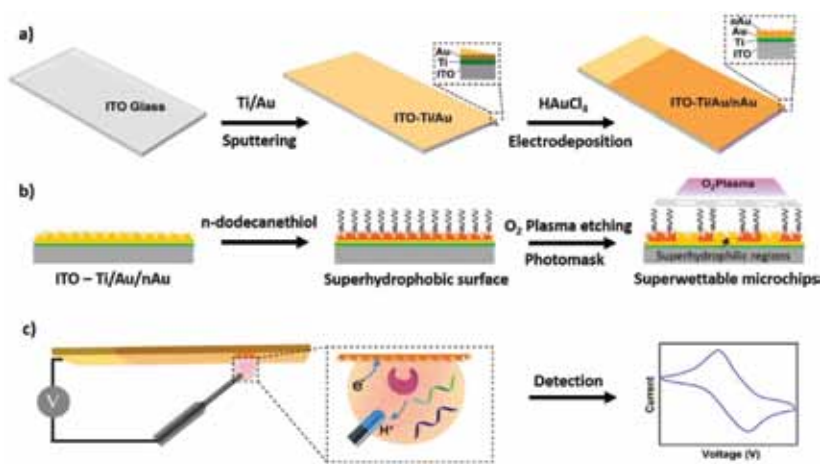


FIGURE 7

The superwettable electrochemical sensors with patterned superhydrophobic and superhydrophilic microarrays. (Reprinted with permission [90]. Copyright 2018, American Chemical Society).

plasma was irradiated for 120 seconds onto the dodecanethiol modified substrate so that the irradiated region became superhydrophilic whereas the non-irradiated region remained as superhydrophobic.

## 4 APPLICATIONS OF WETTABILITY CONTRAST SURFACES

Nature-inspired structural modifications resulted in the fabrication of surfaces that exhibit extreme wettability and such surfaces are finding applications in diverse areas, ranging from self-cleaning surfaces to biomedical sciences. As compared to the surfaces with one kind of wettability behaviour, wettability contrast surfaces offer a means for controlling the wettability behaviour and thus provides new avenues for liquid/droplet transport. Such separation and transportation of the aqueous media via wettability contrast open up a plethora of novel technological applications, ranging from localized cooling, cell growth in a controlled environment, microfluidics, etc. [71, 96-98]. In recent years, the structural design of materials inspired by desert beetle to address the crisis of mankind in areas like water harvesting, anti-icing, single-cell assays, oil-water separation, etc. [71] has been witnessed. Even though a complete, comprehensive review of all the literature reported in the area of desert beetle inspired superhydrophobic-superhydrophilic surfaces are beyond the scope of the present review, a few important applications are outlined in the following sections.

### 4.1 Fog Collection/Water Harvesting

Most of the water harvesting studies using the structural modification to superhydrophobic-superhydrophilic patterns are inspired by the wettability pattern on the backside of the *Stenocara* beetle. Parker *et al.* [69] mimicked the structure of the beetle's backside where the small water droplets in the morning fog accumulate on the random hydrophilic bump region (0.5 mm in size separated at a distance of 0.5 to 1.5 mm) and coalesce to form a big droplet. In the desert, the fog droplet is the only available source of water and its size ranges from 1 to 40  $\mu\text{m}$ , which is much less as compared to the size of rain droplets. When the droplet size is big enough to overcome the binding force of the hydrophilic region, the droplet rolls off through the waxy hydrophobic region ( $\sim 10 \mu\text{m}$  in size) and finally reaches the beetle's mouth providing a fresh morning drink for the beetle. The tilting of the back wings to the fog enables the beetle to collect the water in the hydrophilic region, whereas the fog incident on the hydrophobic region blows towards the hydrophilic region. The naturally occurring micro-condensation surface has been mimicked using random and ordered an array of 0.6 mm glass spheres on a waxy background, and it is seen that an ordered array of spheres provide optimum conditions for micro-condensation [69]. In a work done by Badyal *et al.* [99], they evaluated the micro-condensation efficiency of a variety of hydrophilic-

hydrophobic patterned substrates with respect to their surface functionality and dimension. The study relied on the fabrication of hydrophilic patterned surfaces via  $\text{CF}_4$  or  $\text{O}_2$  plasma onto the superhydrophobic surface (plasma-fluorinated polybutadiene (advancing/receding WCA)  $154^\circ/152^\circ$ ) and plasma etched poly(tetrafluoroethylene) (advancing/receding WCA,  $152^\circ/151^\circ$ ), as depicted in Figure 8.  $500\ \mu\text{m}$  was found to be the optimum size of the hydrophilic spot, and the separation between the hydrophilic spot was estimated as  $1,000\ \mu\text{m}$ . Above the optimum hydrophilic spot size, the droplet could not achieve the critical size of the droplet condensation due to evaporation, and below the critical size, droplets could not overcome surface tension due to insufficient masses. So, the droplet remained in the hydrophilic region in the former case. This chemical method of fabricating superhydrophilic patterns on the superhydrophobic background gave comparable results with the water collection by the beetle's back surface.

Dorrer *et al.* [72] explained the fabrication of a superhydrophobic background with relatively less hydrophobic or hydrophilic bumps by dispensing polymers on the nanograss surface using a pipet. They found that the surface

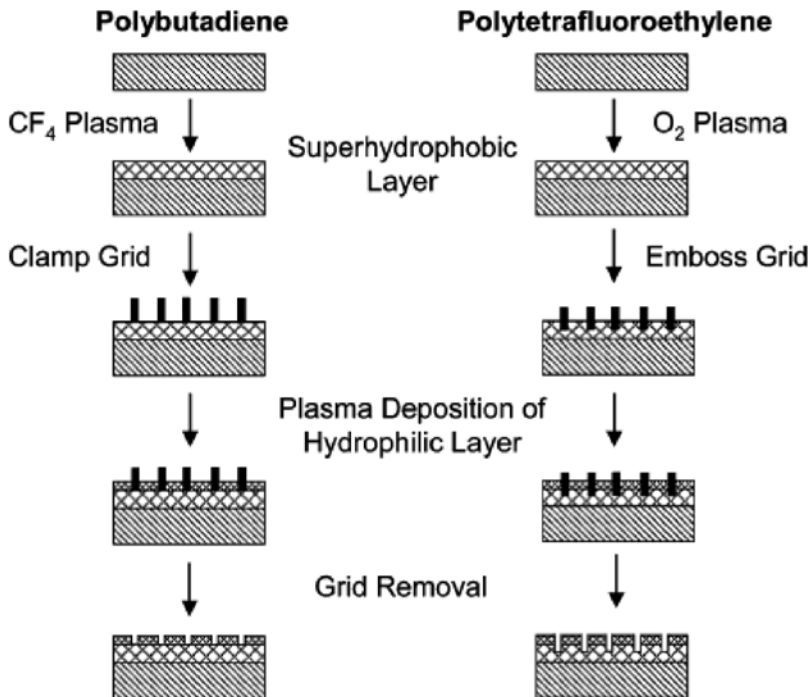


FIGURE 8

Micropatterning hydrophilic plasma polymerizer onto a superhydrophobic background. (Reprinted with permission [93]. Copyright 2007, American Chemical Society).

property became closely equivalent to that of the beetle's back surface. Their model surface covered a range of wettability contrasts between  $178^\circ/0^\circ$  and  $178^\circ/120^\circ$  and investigated the influence of the wettability contrast on the dewetting of drops from the surfaces. 100% mimicking could not be achieved because of the difference in the effective diameter of the hydrophilic bumps and the force of the fog wind in the desert.

The work done by Lei Jiang *et al.* [83] showed bioinspired surfaces with star-shaped wettability patterns where the structural features of beetles' back and spider silk (capability to collect tiny droplets in a directional manner to form large droplets on more wettable regions) were integrated. Upon exposure to fog flow, the fog droplets initially condensed everywhere on the surface, but due to the surface energy gradient, the droplet propelled to the superhydrophobic region. The integration of surface energy gradient and Laplace pressure gradient on these surfaces drive the tiny water droplets quickly into superhydrophilic region. To investigate the water collection efficiency, the Authors investigated five types of surfaces (circle-patterned, 4-, 5-, 6- and 8- pointed star-patterned surfaces) other than uniform hydrophilic/hydrophobic surfaces and compared the water collected per unit time and unit area. In the study, the samples (20 mm x 20 mm) with a pattern size of  $<1000 \mu\text{m}$  were kept at different inclination angles ( $15^\circ$ ,  $45^\circ$  and  $90^\circ$ ) to the horizontal plane under a fog flow rate of  $<75 \text{ cm/s}$ . It was found that the uniformly superhydrophobic surface collected more water than the uniformly superhydrophilic surface ( $\sim 1.33$  and  $\sim 0.55 \text{ g cm}^{-2}\text{h}^{-1}$ , respectively) because the superhydrophobic surface allowed droplets to roll down into the water collecting container more efficiently instead of adhering and evaporating on the superhydrophilic surface. The water collection efficiency of surfaces with circle-shaped patterns was found to be  $\sim 1.65 \text{ g cm}^{-2}\text{h}^{-1}$  whereas the star-shaped patterns exhibited a collection efficiency ranging from 2.11 to  $2.78 \text{ g cm}^{-2}\text{h}^{-1}$ . The droplet rolled under the gravity when the droplet size grew to a critical size in accordance with the relationship  $\rho g V \sin\alpha > w\gamma\cos(\theta_{upper} - \theta_{lower})$ , where  $\rho$  and  $V$  are the density and volume of the droplet,  $g$  is the acceleration due to gravity.  $\alpha$  is the inclination angle,  $w$  is the air-liquid-solid contact line.  $\theta_{upper}$  and  $\theta_{lower}$  are the contact angles at the upper and lower side, respectively. A comparison with circle-shaped patterns, the 5-star shaped patterns always showed higher water collection efficiency for all the inclination angles investigated.

Another interesting study where superhydrophilic micropatterns were induced onto a superhydrophobic surface via facile inkjet printing of dopamine solution [93]. The  $4 \text{ mm}^2$  prepared substrates were vertically placed on a thermoelectric cooling module (temperature  $\sim 4^\circ\text{C}$ ) and exposed to a fog flow ( $\sim 10 \text{ cm/s}$ ). It was found that the polydopamine patterned superhydrophilic region ( $\sim 500 \mu\text{m}$ ) with pattern spacing of  $1000 \mu\text{m}$  exhibited a harvesting efficiency of  $\sim 61.8 \text{ mg cm}^{-2}\text{h}^{-1}$  as compared to the  $\sim 14.9 \text{ mg cm}^{-2} \text{ h}^{-1}$  and  $\sim 30.0 \text{ mg cm}^{-2}\text{h}^{-1}$  of superhydrophilic and superhydrophobic substrates.

Zhu *et al.* [100] report that fog harvesting can be achieved by making superhydrophobic circles on a superhydrophilic background. They created two superhydrophobic patterns with a WCA of  $155.2^\circ$  and roll-off angle of  $8.4^\circ$  by a purely chemical method on a copper surface. The water collection efficiency was tested for different substrates such as uniform superhydrophobicity, uniform superhydrophilicity and the highest water-collecting rate was found for surfaces with superhydrophobic circles on superhydrophilic backgrounds. In addition, the water collection efficiency was checked by keeping the substrate for different inclined angles of  $15^\circ$ ,  $45^\circ$  and  $90^\circ$  to the horizontal plane. The most effective water harvesting property was achieved at a  $90^\circ$  inclined angle ( $1316.9 \text{ mg cm}^{-2}\text{h}^{-1}$ ).

Wang *et al.* [85] fabricated superhydrophobic CuO-x-PFDT on hydrophilic polystyrene sheet lab-based thermal processing technique and explored the water harvesting efficiency. Here, the as-prepared samples kept horizontally to investigate the harvesting efficiency from a stimulated flow of fog (about  $12 \text{ cms}^{-1}$ ) generated from a commercial humidifier. The distance between the fog generator and the sample was kept constant at 7 cm, and the duration of the one cycle was four hours. The studies were carried out at  $22^\circ\text{C}$  and a humidity level of  $\sim 90\text{-}95\%$ . Water droplets collected by the surface are drained by gravity into a container placed on top of a digital balance. The uniformly superhydrophobic CuO-PFDT foil and uniformly hydrophilic PS sheet generated water collection rates of 67 and  $60 \text{ mg cm}^{-2} \text{ h}^{-1}$ , respectively, which were far lower than the CuO-50-PFDT-130 sample with a hydrophilic-superhydrophobic patterned surface. The patterned surface nicely integrated two competing processes of water droplet coalescence (facilitated by hydrophilic region) and droplet removal (benefited from superhydrophobicity). This surface was found to exhibit a water collection rate of  $159 \text{ mg cm}^{-2} \text{ h}^{-1}$ .

Li *et al.* [88] fabricated a superhydrophobic-hydrophilic conical stainless needle and explored the use of these for fog harvesting. A comparison of the fog collection efficiency of the prepared needle was compared using three types of conical structures; uniformly hydrophilic, uniformly hydrophobic, and uniformly superhydrophobic under the same flow fog rate of  $70 \text{ cm/s}$ . It was found that superhydrophobic-hydrophilic conical stainless needle gave rise to a high collection efficiency, whereas the uniformly superhydrophobic cone exhibited the least efficiency.

In a very recent study, a hybrid method of femtosecond laser structuring (central wavelength of 1030 nm, duration of 800 fs, and repetition rate of 400 kHz) and hydrothermal method treatment has been employed to create hierarchical nanoneedle structures which, upon treatment with poly(dimethylsiloxane), gave rise to a superhydrophobic property with a low water sliding angle ( $\sim 3^\circ$ ) and a high water adhesion ability [81]. The structured surface was kept at 10 cm away from the commercial ultrasonic humidifier with a flow rate of  $0.0867 \text{ cm}^3/\text{s}$  and kept at an angle  $45^\circ$ . Compared with the Untreated Ti sample only has a water-harvesting efficiency of about  $247 \text{ mg}\cdot\text{cm}^{-2}\cdot\text{h}^{-1}$ , the efficiency of the

hierarchical structure surface was about 2.2 times the untreated Ti. In another laser patterned substrate fabrication study (520 nm, 380 fs, 200 kHz), the intrinsic wettability of Pyrex wafers changed to superhydrophilic by femtosecond laser structuring ( $<10^\circ$ ) and then Teflon-like polymer (CF<sub>2</sub>)<sub>n</sub> was deposited via plasma process to tailor the surface to superhydrophobic ( $>150^\circ$ ) [79]. Further selective treatment with femtosecond laser was employed to remove the Teflon coating to fabricate a superhydrophobic-superhydrophilic surface. In order to investigate the influence on the fog-collection behavior, (super)hydrophilic, (super)hydrophobic, low, and high contrast wetting patterns are fabricated on glass wafers using all reasonable combinations of these three processing steps and exposed to fog in an artificial nebulizer setup. This experiment revealed that high contrast wetting patterns exhibit the highest amount of fog and the fog-collection efficiency is enhanced nearly by 60% as compared to pristine Pyrex glass.

#### 4.2 Microarray Fabrication

Through thiol-yne click chemistry surface patterning, superhydrophobic-superhydrophilic patterns of well-defined sizes and geometries were prepared by Levkin *et al.* [101] with feature sizes as small as 10  $\mu\text{m}$ . Surfaces with such high wettability contrast and small dimensions are efficiently used to separate microdroplets (Droplet microarray approach). Further, such surfaces are used for cell confinement in that region. In another work, superhydrophobic surfaces were fabricated from the dry power mixtures of hydrophobic silica nanoparticles and toner powders to facilitate the fabrication of superhydrophobic surfaces on a paper and polymer sheets using a commercial laser printer [102]. The wettability contrast between the printed and non-printed regions were exploited for droplet positioning and droplet mixing. In another study, by printing an ethanol solution of phospholipid on a superhydrophobic surface, patterned superhydrophilic regions are made (Figure 9) [103]. The difference in wettability has been exploited to an array of superhydrophilic regions filled with a solution of Rhodamine 6G so that droplet assay was formed, which can be probed further upon evaporation. Levkin *et al.* [74] also demonstrated a facile method for the fabrication of arrays of superhydrophilic microspots separated by superhydrophobic barriers and was exploited to make living cell microarrays that devoid the cross-contamination and cell-migration problems. By using the spontaneous separation due to wettability contrast, the same group also demonstrated another one-step method for creating thousands of isolated microdroplets with defined geometry and volume [104]. Bioactive molecules, nonadherent cells, or microorganisms can be trapped in the fully isolated microdroplets.

#### 4.3 Biomedical Applications

In an interesting application, Piret *et al.* [105] vertically aligned silicon nanowire (SiNW) arrays were prepared by a stain etching technique,

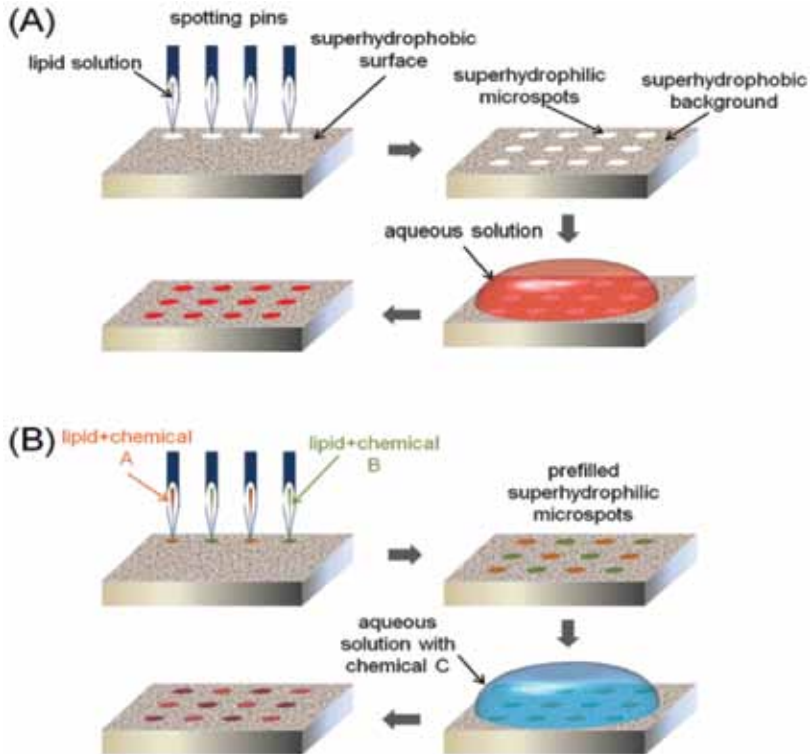


FIGURE 9

(A, B) An example of the application of a microcontact printer to create an array of superhydrophilic microspots on a superhydrophobic background using a lipid/ethanol solution as an ink. (Reprinted with permission [103]. Copyright 2012, American Chemical Society).

which was then chemically modified with octadecyltrichlorosilane (OTS) to obtain a superhydrophobic surface with a WCA  $\sim 160^\circ$ . The surface was then micropatterned to fabricate a superhydrophilic/superhydrophobic SiNW surface via optical lithography. This surface was used to show culturing of Chinese Hamster Ovary K1 (CHO) cell elucidate that cells were selectively adhering to the hydrophilic region. Similarly, the selective adhesion of 3T3 fibroblast cells to superhydrophilic regions as compared to the superhydrophobic region due to protein absorption was demonstrated by Ishizaki *et al.* [73]. Further, they also demonstrated cell-cell direct communication occurring between cells in neighboring patterns with a distance of fewer than  $250 \mu\text{m}$ .

Mano *et al.* [106] demonstrated the fabrication of the wettability contrast surfaces to fix the cell suspension droplets in the wettable regions by three distinct modes: (1) by pipetting the cell suspension directly in each individual spot, (2) by the continuous dragging of a cell suspension on the

chip, and (3) by dipping the whole chip in a cell suspension. The degrees of precision and throughput found to depend upon the method employed, and each spot was exploited as a mini-bioreactor and facilitated image-based on-chip analysis [106]. The same group also developed flat devices for high throughput screening of accelerated evaluation of multiplexed processes and reactions taking place in the aqueous-based environment. This was done by creating rose petal surfaces on a lotus leaf substrate via micro-indentation [107].

#### 4.4 Other applications

Droplet manipulation on hydrophobic/superhydrophobic patterned copper surfaces has been achieved using masks created by simple pen drawing and site-selective nanowire growth in aqueous solution [86]. Ink removal by organic solvents and subsequent deposition of a fluorocarbon thin film resulted in a hydrophobic pattern and a super-hydrophobic background. By controlling the pattern dimensions, anisotropic adhesion of water droplets and consequent directional transport of water droplets in the line and curved patterns were demonstrated, which has applications in open microfluidics and diagnostic platforms. In a very interesting work, Levkin *et al.* [75] demonstrated the idea of creating superhydrophilic spots on the porous polymer surface, which showed superhydrophobic nature, by photo-initiated surface grafting. Because of the three-dimensionality and extreme wettability differences, this method can be used for microfluidic applications.

A flower-like Ag microstructure on PDMS surface was fabricated by dripping 2 mM silver nitrate ( $\text{AgNO}_3$ ) solution onto a cell culture dish followed by pouring PDMS onto it. This provided a facile approach for the detection of SERS (surface-enhanced Raman spectroscopy) signal of DPA from a single cell with a minimum limit of detection of 1.2 pM. Figure 10 shows the schematic diagram of the construction of 3D plasmonic trap array and the 3D trap applied for quantitative real-time SERS monitoring of single-cell secretion. The lower detection limit of aM concentration was obtained for Raman reporter *p*-ATP and with an enhancement factor of  $1.1 \times 10^7$  [108].

Farshchian *et al.* [109] demonstrated the fabrication of moderate and extreme wettability contrast on poly-methyl methacrylate (PMMA) surfaces and carried out an investigation on the droplet impinging effects on such surfaces. To achieve the wettability contrast, hydrophobic polydimethylsiloxane (PDMS) coated nanoparticles were imprinted on the hydrophilic PMMA surface, which contributed to hierarchical roughness on the unmasked PMMA surface. While treating the same with plasma made the surface superhydrophilic, the WCA of the pristine PMMA ( $83 \pm 2^\circ$ ) is enhanced to  $164 \pm 5^\circ$  via the use of nanoparticles. The plasma treatment reduced the WCA to  $9 \pm 1^\circ$ . Moreover, the directional rebounding of water droplets towards the hydrophilic region was also explained.

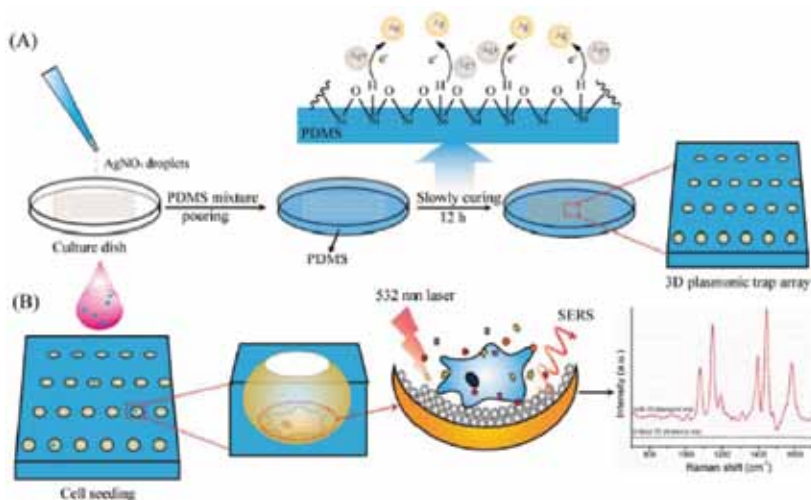


FIGURE 10

A) Schematic Diagram Showing Construction of 3D Plasmonic Trap Array and (B) the 3D Trap Applied for Quantitative Real-Time SERS Monitoring of Single-cell Secretion. (Reprinted with permission [102]. Copyright 2018, American Chemical Society).

## 5 CONCLUSIONS

The research work in the field of fabrication and application of the wettability contrast surface is rapidly progressing. Despite the progress in the fabrication of wettability contrast surfaces via physical and chemical methods, the fabrication of stable and biocompatible wettability contrast surfaces in a cost-effective, easy, and facile route remains a significant challenge. As explained in the review, physical methods like laser patterning are emerging as a favorable approach as compared to the chemical methods, largely due to the inherent advantages associated with laser patterning. Irrespective of the technique adopted, most of the studies rely on the fabrication of hierarchical micro/nanoscale structures to achieve the Cassie-Baxter state to obtain the liquid repellency behavior and hydrophilic regions mostly follow the Wenzel state or Cassie-impregnated state. A plethora of applications have already been demonstrated with such wettability patterned surfaces, with much recent focus on fog/water harvesting and droplet bioassay for biological applications. Also, cell culture in the selective regions has been demonstrated with great efficacy. Aside from the existing wide range of applications, it is expected that wettability contrast surfaces can find more applications in the fields of photonics, wearable sensors, nanotechnology-based devices, etc. Moreover, the application of this kind of surface for *In Vivo* applications remains a formidable task.

## REFERENCES

- [1] Koch K., Bhushan B. and Barthlott W., Diversity of structure, morphology, and wetting of plant surfaces. *Soft Matter* **4** (2008), 1943-1963.
- [2] Koch K. and Barthlott W., Superhydrophobic and superhydrophilic plant surfaces: an inspiration for biomimetic materials. *Philosophical Transactions of the Royal Society A: Mathematical, Physical and Engineering Sciences* **367** (2009), 1487-1509.
- [3] Cho W.K. and Choi I.S., Fabrication of hairy polymeric films inspired by geckos: wetting and high adhesion properties. *Advanced Functional Materials* **18** (2008), 1089-1096.
- [4] Li J., Liu X., Ye Y., Zhou H. and Chen J., Gecko-inspired synthesis of superhydrophobic ZnO surfaces with high water adhesion. *Colloids and Surfaces A: Physicochemical and Engineering Aspects* **384** (2011), 109-114.
- [5] Zheng Y., Gao X. and Jiang L., Directional adhesion of superhydrophobic butterfly wings, *Soft Matter* **3** (2007), 178-182.
- [6] Lu Y., Yu L., Zhang Z., Wu S., Li G., Wu P., Hu Y., Li J., Chu J. and Wu D., Biomimetic surfaces with anisotropic sliding wetting by energy-modulation femtosecond laser irradiation for enhanced water collection. *RSC Advances* **7** (2017), 11170-11179.
- [7] Guo Z. and Liu W., Biomimic from the superhydrophobic plant leaves in nature: Binary structure and unitary structure. *Plant Science* **172** (2007), 1103-1112.
- [8] Barthlott W. and Neinhuis C., Purity of the sacred lotus, or escape from contamination in biological surfaces. *Planta* **202** (1997), 1-8.
- [9] Neinhuis C. and Barthlott W., Characterization and distribution of water-repellent, self-cleaning plant surfaces. *Annals of botany* **79** (1997), 667-677.
- [10] Feng L., Li S., Li Y., Li H., Zhang L., Zhai J., Song Y., Liu B., Jiang L. and Zhu D., Superhydrophobic surfaces: from natural to artificial. *Advanced Materials* **14** (2002), 1857-1860.
- [11] Zheng Y., Han D., Zhai J. and Jiang L., In situ investigation on dynamic suspending of microdroplet on lotus leaf and gradient of wettable micro-and nanostructure from water condensation. *Applied Physics Letters* **92** (2008), 084106.
- [12] Chen P., Chen L., Han D., Zhai J., Zheng Y. and Jiang L., Wetting behavior at micro-/nanoscales: Direct imaging of a microscopic water/air/solid three-phase interface. *Small* **5** (2009), 908-912.
- [13] George J.E., Chidangil S. and George S.D., Recent progress in fabricating superaerophobic and superaerophilic surfaces. *Advanced Materials Interfaces* **4** (2017), 1601088.
- [14] Zhang Y.-L., Wang J.-N., He Y., He Y., Xu B.-B., Wei S. and Xiao F.-S., Solvothermal synthesis of nanoporous polymer chalk for painting superhydrophobic surfaces. *Langmuir* **27** (2011), 12585-12590.
- [15] Jung C.-K., Bae I.-S., Lee S.-B., Cho J.-H., Shin E.-S., Choi S.-C. and Boo J.-H., Development of painting technology using plasma surface technology for automobile parts. *Thin Solid Films* **506** (2006), 316-322.
- [16] Tian D., Song Y. and Jiang L., Patterning of controllable surface wettability for printing techniques. *Chemical Society Reviews* **42** (2013), 5184-5209.
- [17] Nguyen P.Q., Yeo L.-P., Lok B.-K. and Lam Y.-C., Patterned surface with controllable wettability for inkjet printing of flexible printed electronics. *ACS Applied Materials & Interfaces* **6** (2014), 4011-4016.
- [18] Ta D.V., Dunn A., Wasley T.J., Kay R.W., Stringer J., Smith P.J., Connaughton C. and Shephard J.D., Nanosecond laser textured superhydrophobic metallic surfaces and their chemical sensing applications. *Applied Surface Science* **357** (2015), 248-254.
- [19] Sun T., Feng L., Gao X. and Jiang L., Bioinspired surfaces with special wettability. *Accounts of Chemical Research* **38** (2005), 644-652.
- [20] Waugh D.G. and Lawrence J., Towards a technique for controlling wettability characteristics and conditioning film formation on polyethylene terephthalate (PET) through laser surface engineering. *Lasers in Engineering* **37** (2017), 207-232.
- [21] Ng C.-H., *Laser Surface Modification of NiTi for Medical Applications*, University of Chester, United Kingdom, 2017.

- [22] Young T., III. An essay on the cohesion of fluids. *Philosophical Transactions of the Royal Society of London* (1805), 65-87.
- [23] Wang B., Zhang Y., Shi L., Li J. and Guo Z., Advances in the theory of superhydrophobic surfaces. *Journal of Materials Chemistry* **22** (2012), 20112-20127.
- [24] Berg J., *Wettability*. Boca Raton, FL, USA: CRC Press. 1993.
- [25] Hazlett R.D., Fractal applications: wettability and contact angle. *Journal of Colloid and Interface Science* **137** (1990), 527-533.
- [26] Cassie A. and Baxter S., Wettability of porous surfaces. *Transactions of the Faraday Society* **40** (1944), 546-551.
- [27] Picknett R. and Bexon R., The evaporation of sessile or pendant drops in still air. *Journal of Colloid and Interface Science* **61** (1977), 336-350.
- [28] Li Q., Zhou P. and Yan H., Pinning–depinning mechanism of the contact line during evaporation on chemically patterned surfaces: a lattice Boltzmann study. *Langmuir* **32** (2016), 9389-9396.
- [29] Eustathopoulos N., Nicholas M.G. and Drevet B., *Wettability at High Temperatures*. London, UK: Elsevier. 1999.
- [30] Sun Y. and Guo Z., Recent advances of bioinspired functional materials with specific wettability: from nature and beyond nature. *Nanoscale Horizons* **4** (2019), 52-76.
- [31] Ali J.A., Kolo K., Manshad A.K. and Mohammadi A.H., Recent advances in application of nanotechnology in chemical enhanced oil recovery: Effects of nanoparticles on wettability alteration, interfacial tension reduction, and flooding. *Egyptian Journal of Petroleum* **27** (2018), 1371-1383.
- [32] Brutin D. and Starov V., Recent advances in droplet wetting and evaporation. *Chemical Society Reviews* **47** (2018), 558-585.
- [33] Siddiqui M.A.Q., Ali S., Fei H. and Roshan H., Current understanding of shale wettability: A review on contact angle measurements. *Earth-Science Reviews* **181** (2018), 1-11.
- [34] Kassa A., Gasda S., Kumar K. and Radu F., Impact of time-dependent wettability alteration on dynamic capillary pressure. *The 5th CO2 Geological Storage Workshop, European Association of Geoscientists & Engineers*. 2018, pp. 1-5.
- [35] Patankar N.A., Mimicking the lotus effect: influence of double roughness structures and slender pillars. *Langmuir* **20** (2004), 8209-8213.
- [36] Shibuichi S., Onda T., Satoh N. and Tsujii K., Super water-repellent surfaces resulting from fractal structure, *The Journal of Physical Chemistry*, 100 (1996) 19512-19517.
- [37] Shibuichi S., Yamamoto T., Onda T. and Tsujii K., Super water-and oil-repellent surfaces resulting from fractal structure. *Journal of Colloid and Interface Science* **208** (1998), 287-294.
- [38] Vincent J.F., Bogatyreva O.A., Bogatyrev N.R., Bowyer A. and Pahl A.-K., Biomimetics: its practice and theory. *Journal of the Royal Society Interface* **3** (2006), 471-482.
- [39] McCarty M., Life of bionics founder a fine adventure, *Dayton Daily News* (2009).
- [40] Lin J., Cai Y., Wang X., Ding B., Yu J. and Wang M., Fabrication of biomimetic superhydrophobic surfaces inspired by lotus leaf and silver ragwort leaf. *Nanoscale* **3** (2011), 1258-1262.
- [41] Sun M., Watson G.S., Zheng Y., Watson J.A. and Liang A., Wetting properties on nanostructured surfaces of cicada wings. *Journal of Experimental Biology* **212** (2009), 3148-3155.
- [42] Kelleher S.M., Habimana O., Lawler J., O'reilly B., Daniels S., Casey E. and Cowley A., Cicada wing surface topography: an investigation into the bactericidal properties of nanostructural features. *ACS Applied Materials & Interfaces* **8** (2015), 14966-14974.
- [43] Waghmare P.R., Gunda N.S.K. and Mitra S.K., Under-water superoleophobicity of fish scales. *Scientific Reports* **4** (2014), 7454 1-5.
- [44] Birjandi F.C. and Sargolzaei J., Super-non-wettable surfaces: A review. *Colloids and Surfaces A: Physicochemical and Engineering Aspects* **448** (2014), 93-106.
- [45] George J.E., Rodrigues V.R., Mathur D., Chidangil S. and George S.D., Self-cleaning superhydrophobic surfaces with underwater superaerophobicity. *Materials & Design* **100** (2016), 8-18.

- [46] George J.E., Chidangil S. and George S.D., A study on air bubble wetting: Role of surface wettability, surface tension, and ionic surfactants. *Applied Surface Science* **410** (2017), 117-125.
- [47] George J.E., Unnikrishnan V., Mathur D., Chidangil S. and George S.D., Flexible superhydrophobic SERS substrates fabricated by in situ reduction of Ag on femtosecond laser-written hierarchical surfaces. *Sensors and Actuators B: Chemical* **272** (2018), 485-493.
- [48] Waugh D.G. and Lawrence J., On the use of CO<sub>2</sub> laser induced surface patterns to modify the wettability of poly (methyl methacrylate)(PMMA). *Optics and Lasers in Engineering* **48** (2010), 707-715.
- [49] Liu M., Wang S. and Jiang L., Bioinspired multiscale surfaces with special wettability. *MRS Bulletin* **38** (2013), 375-382.
- [50] Niu S., Li B., Mu Z., Yang M., Zhang J., Han Z. and Ren L., Excellent structure-based multifunction of Morpho butterfly wings: A review. *Journal of Bionic Engineering* **12** (2015), 170-189.
- [51] Pu X., Li G. and Huang H., Preparation, anti-biofouling and drag-reduction properties of a biomimetic shark skin surface. *Biology Open* **5** (2016), 389-396.
- [52] Bixler G.D. and Bhushan B., Rice and butterfly wing effect inspired low drag and antifouling surfaces: a review. *Critical Reviews in Solid State and Materials Sciences* **40** (2015), 1-37.
- [53] Lee Y., Ju K.-Y. and Lee J.-K., Stable biomimetic superhydrophobic surfaces fabricated by polymer replication method from hierarchically structured surfaces of Al templates. *Langmuir* **26** (2010), 14103-14110.
- [54] Pozzato A., Dal Zilio S., Fois G., Vendramin D., Mistura G., Belotti M., Chen Y. and Natali M., Superhydrophobic surfaces fabricated by nanoimprint lithography. *Microelectronic Engineering* **83** (2006), 884-888.
- [55] Qian B. and Shen Z., Fabrication of superhydrophobic surfaces by dislocation-selective chemical etching on aluminum, copper, and zinc substrates. *Langmuir* **21** (2005), 9007-9009.
- [56] Wang S., Liu C., Liu G., Zhang M., Li J. and Wang C., Fabrication of superhydrophobic wood surface by a sol-gel process. *Applied Surface Science* **258** (2011), 806-810.
- [57] Ma M. and Hill R.M., Superhydrophobic surfaces. *Current Opinion in Colloid & Interface Science* **11** (2006), 193-202.
- [58] Wang X., Ding B., Yu J. and Wang M., Engineering biomimetic superhydrophobic surfaces of electrospun nanomaterials. *Nano Today* **6** (2011), 510-530.
- [59] Li Y., Liu F. and Sun J., A facile layer-by-layer deposition process for the fabrication of highly transparent superhydrophobic coatings. *Chemical Communications* (2009), 2730-2732.
- [60] Rezaei S., Manoucheri I., Moradian R. and Pourabbas B., One-step chemical vapor deposition and modification of silica nanoparticles at the lowest possible temperature and superhydrophobic surface fabrication. *Chemical Engineering Journal* **252** (2014), 11-16.
- [61] Song X., Zhai J., Wang Y. and Jiang L., Fabrication of superhydrophobic surfaces by self-assembly and their water-adhesion properties. *The Journal of Physical Chemistry B* **109** (2005), 4048-4052.
- [62] Baldacchini T., Carey J.E., Zhou M. and Mazur E., Superhydrophobic surfaces prepared by microstructuring of silicon using a femtosecond laser. *Langmuir* **22** (2006), 4917-4919.
- [63] Drelich J., E. Chibowski, D.D. Meng, K. Terpilowski, Hydrophilic and superhydrophilic surfaces and materials, *Soft Matter*, 7 (2011) 9804-9828.
- [64] Liu H., Feng L., Zhai J., Jiang L. and Zhu D., Reversible wettability of a chemical vapor deposition prepared ZnO film between superhydrophobicity and superhydrophilicity. *Langmuir* **20** (2004), 5659-5661.
- [65] Zhang W., Zhu Y., Liu X., Wang D., Li J., Jiang L. and Jin J., Salt-induced fabrication of superhydrophilic and underwater superoleophobic PAA-g-PVDF membranes for effective separation of oil-in-water emulsions. *Angewandte Chemie International Edition* **53** (2014), 856-860.
- [66] Özgür C. and Şan O., Fabrication of superhydrophilic membrane filters using spherical glass particles obtained by ultrasonic spray pyrolysis. *Ceramics International* **37** (2011), 965-970.

- [67] Otitoju T., Ahmad A. and Ooi B., Superhydrophilic (superwetting) surfaces: A review on fabrication and application. *Journal of Industrial and Engineering Chemistry* **47** (2017), 19-40.
- [68] Zhang L., Zhao N. and Xu J., Fabrication and application of superhydrophilic surfaces: a review. *Journal of Adhesion Science and Technology* **28** (2014), 769-790.
- [69] A.R. Parker, C.R. Lawrence, Water capture by a desert beetle, *Nature*, 414 (2001) 33-34.
- [70] Yu Z., Yun F.F., Wang Y., Yao L., Dou S., Liu K., Jiang L. and Wang X., Desert beetle inspired superwetttable patterned surfaces for water harvesting. *Small* **13** (2017), 1701403 1-6.
- [71] Zhu H., Huang Y., Lou X. and Xia F., Beetle-inspired wetttable materials: From fabrications to applications. *Materials Today Nano* **6** (2019), 100034.
- [72] Dorrer C. and Rhe J.r., Mimicking the Stenocara beetle: Dewetting of drops from a patterned superhydrophobic surface. *Langmuir* **24** (2008), 6154-6158.
- [73] Ishizaki T., Saito N. and Takai O., Correlation of cell adhesive behaviors on superhydrophobic, superhydrophilic, and micropatterned superhydrophobic/superhydrophilic surfaces to their surface chemistry. *Langmuir* **26** (2010), 8147-8154.
- [74] Geyer F.L., Ueda E., Liebel U., Grau N. and Levkin P.A., Superhydrophobic–superhydrophilic micropatterning: towards genome-on-a-chip cell microarrays. *Angewandte Chemie International Edition* **50** (2011), 8424-8427.
- [75] Zahner D., Abagat J., Svec F., Frchet J.M. and Levkin P.A., A facile approach to superhydrophilic–superhydrophobic patterns in porous polymer films. *Advanced Materials* **23** (2011), 3030-3034.
- [76] Huang Y., Hu Y., Zhu C., Zhang F., Li H., Lu X. and Meng S., Long-lived multifunctional superhydrophobic heterostructure via molecular self-supply. *Advanced Materials Interfaces* **3** (2016), 1500727.
- [77] Chitnis G., Ding Z., Chang C.-L., Savran C.A. and Ziaie B., Laser-treated hydrophobic paper: an inexpensive microfluidic platform. *Lab on a Chip* **11** (2011), 1161-1165.
- [78] Yu Z., Yun F.F., Wang Y., Yao L., Dou S., Liu K., Jiang L. and Wang X., Desert beetle inspired superwetttable patterned surfaces for water harvesting. *Small* **13** (2017), 1701403.
- [79] Kostal E., Stroj S., Kasemann S., Matylitsky V. and Domke M., Fabrication of biomimetic fog-collecting superhydrophilic–superhydrophobic surface micropatterns using femtosecond lasers. *Langmuir* **34** (2018), 2933-2941.
- [80] Assaf Y., Forstmann G. and Kietzig A.-M., Wettability modification of porous PET by atmospheric femtosecond PLD. *Applied Surface Science* **436** (2018), 1075-1082.
- [81] Lu J., Ngo C.-V., Singh S.C., Yang J., Xin W., Yu Z. and Guo C., Bioinspired hierarchical surfaces fabricated by femtosecond laser and hydrothermal method for water harvesting. *Langmuir* **35** (2019), 3562-3567.
- [82] Zhai L., Berg M.C., Cebeci F.C., Kim Y., Milwid J.M., Rubner M.F. and Cohen R.E., Patterned superhydrophobic surfaces: toward a synthetic mimic of the Namib Desert beetle. *Nano Letters* **6** (2006), 1213-1217.
- [83] Bai H., Wang L., Ju J., Sun R., Zheng Y. and Jiang L., Efficient water collection on integrative bioinspired surfaces with star-shaped wettability patterns. *Advanced Materials* **26** (2014), 5025-5030.
- [84] Zhang L., Yu H., Zhao N., Dang Z.M. and Xu J., Patterned polymer surfaces with wetting contrast prepared by polydopamine modification. *Journal of Applied Polymer Science* **131** (2014), 41057–41062.
- [85] Wang Y., Zhang L., Wu J., Hedhili M.N. and Wang P., A facile strategy for the fabrication of a bioinspired hydrophilic–superhydrophobic patterned surface for highly efficient fog-harvesting. *Journal of Materials Chemistry A* **3** (2015), 18963-18969.
- [86] Choi W.T., Yang X., Breedveld V. and Hess D.W., Creation of wettability contrast patterns on metallic surfaces via pen drawn masks. *Applied Surface Science* **426** (2017), 1241-1248.
- [87] Huang S., Zheng H., Liu J., Song J., Chen F., Yang X., Sun J., Xu W. and Liu X., Fabrication of extreme wettability patterns with water-film protection for organic liquids. *Journal of Dispersion Science and Technology* **38** (2017), 566-569.

- [88] Chen D., Li J., Zhao J., Guo J., Zhang S., Sherazi T.A. and Li S., Bioinspired superhydrophilic-superhydrophobic integrated surface with conical pattern-shape for self-driven fog collection. *Journal of Colloid and Interface Science* **530** (2018), 274-281.
- [89] Kim S., Moon M.-W. and Kim H.-Y., Drop impact on super-wettability-contrast annular patterns. *Journal of Fluid Mechanics* **730** (2013), 328-342.
- [90] Xu L.P., Chen Y., Yang G., Shi W., Dai B., Li G., Cao Y., Wen Y., Zhang X. and Wang S., Ultratrace DNA detection based on the condensing-enrichment effect of superwettability microchips. *Advanced Materials* **27** (2015), 6878-6884.
- [91] Chen Y., Min X., Zhang X., Zhang F., Lu S., Xu L.-P., Lou X., Xia F., Zhang X. and Wang S., AIE-based superwettability microchips for evaporation and aggregation induced fluorescence enhancement biosensing. *Biosensors and Bioelectronics* **111** (2018), 124-130.
- [92] Schutzius T.M., Graeber G., Elsharkawy M., Oreluk J. and Megaridis C.M., Morphing and vectoring impacting droplets by means of wettability-engineered surfaces. *Scientific Reports* **4** (2014), 7029.
- [93] Zhang L., Wu J., Hedhili M.N., Yang X. and Wang P., Inkjet printing for direct micropatterning of a superhydrophobic surface: toward biomimetic fog harvesting surfaces. *Journal of Materials Chemistry A* **3** (2015), 2844-2852.
- [94] Her E.K., Ko T.-J., Lee K.-R., Oh K.H. and Moon M.-W., Bioinspired steel surfaces with extreme wettability contrast. *Nanoscale* **4** (2012), 2900-2905.
- [95] Xu T., Song Y., Gao W., Wu T., Xu L.-P., Zhang X. and Wang S., Superwettability electrochemical biosensor toward detection of cancer biomarkers. *ACS Sensors* **3** (2018), 72-78.
- [96] George S.D., Ladiwala U., Thomas J., Bankapur A., Chidangil S. and Mathur D., Deposition and alignment of cells on laser-patterned quartz. *Applied Surface Science* **305** (2014), 375-381.
- [97] Banuprasad T.N., Vinay T.V., Subash C.K., Varghese S., George S.D. and Varanakkottu S.N., Fast transport of water droplets over a thermo-switchable surface using rewritable wettability gradient. *ACS Applied Materials & Interfaces* **9** (2017), 28046-28054.
- [98] Mampallil D. and George S.D., Microfluidics—a lab in your palm. *Resonance* **17** (2012), 682-690.
- [99] Garrod R., Harris L., Schofield W., McGettrick J., Ward L., Teare D. and Badyal J., Mimicking a *Stenocara* beetle's back for microcondensation using plasmachemical patterned superhydrophobic-superhydrophilic surfaces. *Langmuir* **23** (2007), 689-693.
- [100] Zhu H., Yang F., Li J. and Guo Z., High-efficiency water collection on biomimetic material with superwettability patterns. *Chemical Communications* **52** (2016), 12415-12417.
- [101] Feng W., Li L., Ueda E., Li J., Heißler S., Welle A., Trapp O. and Levkin P.A., Surface patterning via thiol-yne click chemistry: An extremely fast and versatile approach to superhydrophilic-superhydrophobic micropatterns. *Advanced Materials Interfaces* **1** (2014), 1400269.
- [102] Ngo C.-V. and Chun D.-M., Laser printing of superhydrophobic patterns from mixtures of hydrophobic silica nanoparticles and toner powder. *Scientific Reports* **6** (2016), 36735.
- [103] Li J.S., Ueda E., Nallapaneni A., Li L.X. and Levkin P.A., Printable superhydrophilic-superhydrophobic micropatterns based on supported lipid layers. *Langmuir* **28** (2012), 8286-8291.
- [104] Ueda E., Geyer F.L., Nedashkivska V. and Levkin P.A., DropletMicroarray: facile formation of arrays of microdroplets and hydrogel micropads for cell screening applications. *Lab on a Chip* **12** (2012), 5218-5224.
- [105] Piret G., Coffinier Y., Roux C., Melnyk O. and Boukherroub R., Biomolecule and nanoparticle transfer on patterned and heterogeneously wetted superhydrophobic silicon nanowire surfaces. *Langmuir* **24** (2008), 1670-1672.
- [106] Oliveira M.B., Neto A.I., Correia C.R., Rial-Hermida M.I., Alvarez-Lorenzo C. and Mano J.F., Superhydrophobic chips for cell spheroids high-throughput generation and drug screening. *ACS Applied Materials & Interfaces* **6** (2014), 9488-9495.
- [107] Neto A.I., Correia C.R., Custódio C.A. and Mano J.F., Biomimetic miniaturized platform able to sustain arrays of liquid droplets for high-throughput combinatorial tests. *Advanced Functional Materials* **24** (2014), 5096-5103.

- [108] Yao Y., Ji J., Zhang H., Zhang K., Liu B. and Yang P., Three-dimensional Plasmonic trap Array for ultrasensitive surface-enhanced Raman scattering analysis of single cells. *Analytical Chemistry* **90** (2018), 10394-10399.
- [109] Farshchian B., Pierce J., Beheshti M.S., Park S., and Kim N., Droplet impinging behavior on surfaces with wettability contrasts. *Microelectronic Engineering*, **195** (2018), 50-56.